Ecological Indicators 94 (2018) 430–445

Contents lists available at ScienceDirect

Ecological Indicators

journal homepage: www.elsevier.com/locate/ecolind

Original Articles

Projections of future land use changes: Multiple scenarios-based impacts analysis on ecosystem services for Wuhan city, China

Ying Wang[a], Xiangmei Li[b,*], Qi Zhang[c], Jiangfeng Li[a,*], Xuewu Zhou[a]

[a] School of Public Administration, China University of Geosciences, Wuhan 430074, China
[b] School of Low Carbon Economics, Hubei University of Economics, Wuhan 430205, China
[c] Department of Geography, University of North Carolina at Chapel Hill, Chapel Hill, NC 27599, USA

ARTICLE INFO

Keywords:
Structural optimization
Spatial allocation
Ecosystem services trade-offs
Multi-Objective Programming (MOP)
Dyna-CLUE model
Multiple scenario analysis

ABSTRACT

Urbanization alters the supply of ecosystem services that are vital for human well-being. The loss of ecosystem services is particularly challenging in rapid urbanization areas where economic development needs to consume substantial natural resources. The quantitative and spatial optimization of land use provides an effective tool for rationally allocating land use structure and pattern to ensure the provision of expected ecosystem services. In this paper, we combine the Multi-Objective Programming and the Dyna-CLUE model to project land use changes in 2030 for Wuhan city under three scenarios, i.e., Business As Usual (BAU), Rapid Economic Development (RED), and Ecological Land Protection (ELP). The coupled model that integrates "top-down" and "bottom-up" processes is capable of obtaining the optimized land use patterns under different scenarios and examining the potential impacts of land use changes on ecosystem services in a spatially explicit way. We find that built-up land will continue its remarkable growth during 2015-2030 under the BAU scenario (grows by 96%) at the expense of ecological lands (decreases by 18%). Meanwhile, the predicted losses of ecological lands are 11% and 6% under the RED and ELP scenarios, respectively. Projected land use changes result in varying magnitudes of declines in ecosystem service values for BAU (11%), RED (6%) and ELP (2%) scenarios from 2015 to 2030. The ELP scenario, which incorporates ecological protection policies and spatial restrictions, plays a positive role in altering land use trends and mitigating ecosystem degradation. Finally, we establish an ecosystem service value change matrix to explain how interactions between land use types give rise to trade-offs among multiple ecosystem services. We find that conversions between ecological land use types can trigger trade-offs among ecosystem services, but the conversion from ecological lands towards urban land leads to a net loss of all individual ecosystem services. By linking land and ecological systems, the coupled modeling framework in this study can be useful for obtaining optimal ecosystem-based land use allocation strategies and provide scientific support for sustainable land use management.

1. Introduction

Humans consume a wide range of goods and services provided by ecosystems for survival and welfare (Costanza et al., 1997; Daily et al., 1997). Meanwhile, humans also modify ecosystems over time, intending to enhance the provision of certain types of ecosystem services (ES) to satisfy immediate human needs, such as food, fuel, and shelter (Foley et al., 2005), but often result in losses of other types of ES unintentionally (Defries et al., 2004). In the past few decades, driven by the growing needs arising from population growth, rapid urbanization and economic development, humans have changed ecosystems more drastically and extensively than ever before, e.g., over 60% of global ecosystems have been degraded (MEA, 2005), leading to substantial and largely irreversible loss of ES. Among all human activities, land use/land cover (LULC) change is most relevant to variations in the provision of multiple ES (Lawler et al., 2014), as certain ES are closely tied to specific types of LULC (Costanza et al., 1997; Rodríguez et al., 2006), e.g., timber and climate regulation are mostly provided by forests. Therefore, understanding the linkage between LULC and ES is of key interest to both researchers and policy-makers worldwide.

Studies have made advances in modeling LULC changes (e.g., Azadi et al., 2017), evaluating ES values (e.g., Costanza et al., 2014), and examining responses of ES to LULC dynamics (e.g., Newbold et al., 2015). These studies highlight the profound influences of LULC changes on the provision of ES. For example, the conversion from ecological lands towards urban land can disrupt surface water balance, increase

* Corresponding authors.
E-mail addresses: xmlihust@aliyun.com (X. Li), jfli0524@163.com (J. Li).

https://doi.org/10.1016/j.ecolind.2018.06.047
Received 1 December 2016; Received in revised form 19 June 2018; Accepted 21 June 2018
Available online 17 July 2018

greenhouse gas emissions, and influence regional climate (Foley et al., 2005). The impacts of LULC changes on ES vary widely across different biophysical or socioeconomic settings (Defries et al., 2004), and across different spatial or temporal scales (Clough et al., 2016). Recent research demonstrates that multiple services provided by ecosystems are not independent of each other (Rodríguez et al., 2006). Hence, LULC changes aiming to maximize one particular type of ES may lead to losses of other types of ES, suggesting the existence of trade-offs in the provision of ES (Haase et al., 2012; Rodríguez et al., 2006). Though invisible, trade-offs among multiple ES are taking place all the time, which are often poorly taken into account and thus may cause unintended environmental consequences. Therefore, empirical knowledge of how interactions between LULC types bring about trade-offs among multiple ES is needed for sustainable management of ecosystems.

The relationship between ES and LULC highlights the role of ES in guiding land use planning and decision-making to develop sound management strategies (DeFries et al., 2004). Specifically, ES can be integrated into land use planning in two ways, i.e., serving as an objective of land use optimization models to propose ecologically-friendly land use schemes, or being used for evaluating, comparing, and selecting land use schemes under multiple planning scenarios. For example, Chuai et al. (2013) developed a land use optimization model with the goal of increasing terrestrial ecosystem carbon storage. The model obtained a land use scheme that can bring about a 2% relative increase in carbon storage from 2005 to 2020. Birch et al. (2010) designed three ecosystem restoration scenarios with different discount rates and performed a cost–benefit analysis to identify the best scheme that produces the highest increase in ES with the lowest cost. In this study, ES are used in both ways to inform land use planning, including the design of an “Ecological Land Protection” scenario, and the evaluation of ecosystem responses to land use changes.

Land use optimization models involve complicated processes with competing objectives (Liu et al., 2015a). Existing approaches that simulate these processes can be divided into two categories: bottom-up and top-down. The Multi-Objective Programming (MOP), a top-down approach, is useful for solving problems with conflicting objectives in complex land systems, particularly when incorporating macroeconomic policies (Sadeghi et al., 2009). However, the MOP cannot handle spatial optimization. The Cellular Automata, which is a bottom-up approach, is capable of generating optimized land use spatial patterns (Wang et al., 2015), but it often relies on other models to design conversion rules. The Ant Colony Optimization is a bottom-up approach that solves optimization problems through feedbacks among “ants” (Liu et al., 2008), but it fails to capture the spatial dynamic and heterogeneity of the environment. Most of these optimization models focus on only one aspect, either quantitative optimization of land use structures or spatial optimization of land use patterns, which have limitations. For example, it may not be possible to allocate the optimized land use structure to a specific location due to spatial restrictions, and the aggregated land area from allocated spatial patterns may fail to meet the requirements of different economic sectors. Therefore, it is necessary to adopt a coupled model to optimize both land use quantitative structure and spatial pattern from the top-down and bottom-up perspectives, simultaneously.

In this paper, we propose a coupled model based on the MOP algorithm and the Dynamic Conversion of Land Use and its Effects (Dyna-CLUE) model to simulate land use changes under three scenarios, i.e., Business As Usual (BAU), Rapid Economic Development (RED), and Ecological Land Protection (ELP). The MOP algorithm seeks optimized solutions for each land use type subject to a series of constraints specified by a given scenario. The Dyna-CLUE model, which is dynamic and spatially explicit, allocates the predicted land use changes to grid cells following a bottom-up process (Verburg and Overmars, 2009). The process determines the most suitable land use for each grid cell based on location contexts, the total area of each land use type (derived from the MOP), and a set of rules of spatial restriction (e.g., nature reserves) (Verburg et al., 2012). The combination of the MOP and the Dyna-CLUE makes it possible to optimize the land use quantitative structure and allocate corresponding land use changes to the most suitable location.

Measuring the economic value of ES provides a basis for the inclusion of ES in land use planning and the quantification of ecosystem responses to land use changes. Methods of ES valuation can be divided into two primary types. The first type involves data-based approaches, which combine ecological models and primary data to quantify ecosystem processes and functions that underlie ES, and then convert the derived ES into market prices (Martínez-Harms and Balvanera, 2012). The data-based approaches are data-demanding and complex, and thus are often applied in small-scale studies that focus on a few types of ES. The second type includes the proxy-based approaches, which rely on “benefits transfer” with secondary data such as LULC information (Eigenbrod et al., 2010; Plummer, 2009). For example, the estimated value for each land use type can be transferred from one location to another with similar conditions (Costanza et al., 1997). Although lacking consideration of ES variations over space and time (Eigenbrod et al., 2010; Plummer, 2009; Song et al., 2015), the proxy-based methods are more commonly used due to simplicity and the widespread availability of LULC data. This study adopts the proxy-based approach for the valuation of ES, because it is effective to model the trade-offs among multiple ES arise from land use changes. Moreover, it facilitates the spatial representation of ES, including the spatial distribution of each individual type of ES, and key areas that undergo trade-offs among ES (Martínez-Harms et al., 2016). Finally, this approach is also useful to compare the costs and benefits of ecosystem-based management among different scenarios, which can be difficult for the data-based approach when future data are unavailable.

In this paper, we present a case study in a megalopolis in China to investigate how land use changes under different scenarios will affect the provision of ES by combing a coupled land use optimization model and a proxy-based ES valuation model. Specific objectives include (1) exploring the spatial determinants of the occurrence of each land use type based on a spatial logistic regression model; (2) predicting the spatial-temporal dynamics of land use in 2030 using the coupled MOP and Dyna-CLUE model under three different scenarios, i.e., BAU, RED, and ELP; (3) assessing the effects of land use dynamics on total ES values and trade-offs among multiple ES under the three scenarios.

2. Study area

Wuhan city, the capital of Hubei Province, is located in the middle reaches of the Yangtze River. The city is comprised of thirteen administrative districts (seven urban districts and six rural districts), covering an area of ~8450 km^2 between latitudes of 29°58′–31°22′ N and longitudes of 113°41′–115°05′ E (Fig.1). Wuhan city experiences a subtropical humid monsoon climate, with a mean annual temperature of 15.8–17.5 °C and a mean annual precipitation of 1150–1450 mm. Flat plains (< 100 m) dominate the terrain of Wuhan, while mountains (> 500 m) are mainly located in the northwestern and northeastern parts of the city. We can observe a few low hills in central and southern parts of the city. The forests are mainly distributed in these hilly areas. In addition, surface water accounts for a substantial area of Wuhan (approximately 26%), primarily concentrated in the central part of the city, forming large urban lakes such as East Lake, South Lake and Sha Lake.

Wuhan city is a megalopolis in Central China with a total population of 10.61 million. The Gross Domestic Product (GDP) reached 1,100 billion Chinese Yuan (CNY) in 2015, which ranked eighth among all the cities in China. During 2000 to 2015, Wuhan city has been experiencing accelerated urbanization, leading to extensive expansion of built-up land (from 65,864 ha to 136,277 ha) encroaching the surrounding ecological lands (i.e., cropland, woodland, grassland and water areas). From 2000 to 2015, the total area of ecological lands in Wuhan has decreased by 8%, and the areas of cropland, woodland, grassland

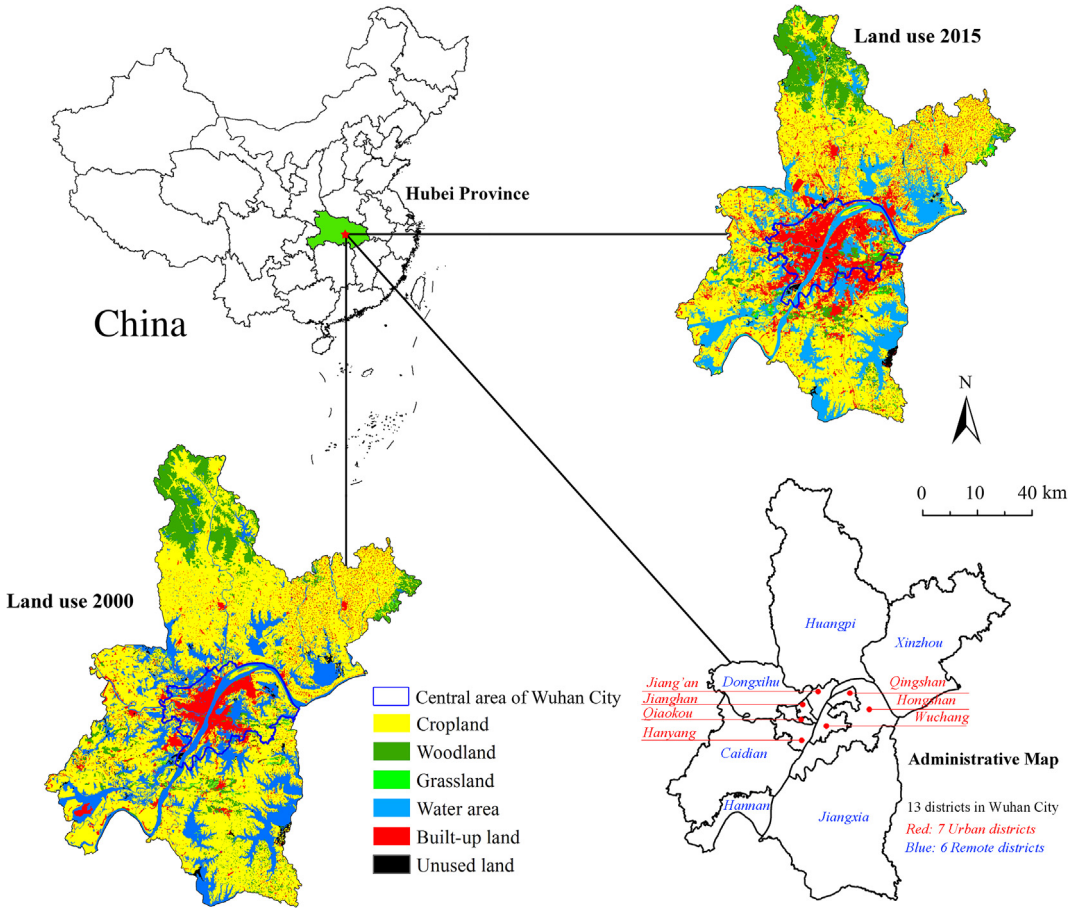

Fig. 1. Study area: geographic location, land use and administrative districts of Wuhan City.

shrunk by 13%, 4% and 2%, respectively (Li et al., 2016).

3. Materials and methods

3.1. Data and processing

Remotely sensed data of Landsat imagery (https://www.usgs.gov/) are used to generate land use maps for 2000, 2005, 2010, and 2015. We also derive the NDVI map in 2015 from the Landsat imagery data. We adopt the classification scheme developed by the Chinese Academy of Sciences (Liu et al., 2013) and identify six land use types, including cropland, woodland, grassland, water area, built-up land, and unused land. Specifically, linear surface features (e.g., roads, streams, and shelter-forest belts), which can be hardly interpreted from Landsat images (30 m resolution) are derived from a land use map produced by the second national land survey of China in 2009. We also collect ground truth points from the map to assess the accuracy of land use classification. The overall accuracies for the classified maps in 2000, 2005, 2010, and 2015 are 76%, 80%, 84%, and 74%, respectively (see Table S1 for a confusion matrix). Other spatial data include the SRTM Digital Elevation Models (DEM) by NASA (https://www2.jpl.nasa.gov/srtm/), and raster maps of soil erosion, soil texture (i.e., clay, sand and silt contents), precipitation, GDP density and population distribution provided by the Data Center for Resources and Environmental Sciences of the Chinese Academy of Sciences (http://www.resdc.cn). All maps are converted to layers with an extent of 1246 × 1529 grid cells and a spatial resolution of 100 m × 100 m in ArcGIS 10.3. Finally, all datasets are extracted by a boundary layer to obtain the data within the study area.

In addition to spatial data, statistical data (e.g., population, GDP, economic benefits of different land types, and labor engaged in various sectors) are collected from historical statistical bureau of Wuhan city (www.stats-hb.gov.cn). Table 1 lists the data sources and preprocessing procedures of the data in this study.

3.2. The coupled land use change model

To simulate land use change trajectories in a spatially explicit manner, we propose an integrated approach that couples the MOP model and the Dyna-CLUE model, which is applied for the three scenarios (i.e., BAU, RED and ELP). The coupled model involves two procedures. First, the MOP algorithm is applied to obtain the land use structural optimization solution (called land use demand) by addressing constrained optimization problems. Second, the predicted trends and quantity of land use changes are spatially allocated to specific locations by the Dyna-CLUE model, depending on the site characteristics and suitability for distinctive land use types, the neighborhood relationships, and the spatial policies and restrictions (Verburg and Overmars, 2009). Fig. 2 provides the framework of our coupled model including the procedures of MOP and Dyna-CLUE.

3.2.1. MOP algorithm: land use structure optimization

We use the MOP algorithm with Lingo 10.0 software to predict the area change of each land use type in 2030 under three scenarios, i.e., BAU, RED, and ELP.

3.2.1.1. Scenarios design. It is always challenging for policy-makers to harmonize economic development and ecological protection. Here, we design three land use scenarios in Wuhan city to inform more appropriate recommendations for policy design and implementation.

Table 1
Data sources and processing.

Main theme	Sub-themes	Year(s)	Spatial resolution	Sources and data preprocessing
Land dataset	Land use and land cover	2000, 2005, 2010, 2015	30 m	Landsat images (path/row 122/39, 123/38, 123/39) obtained from USGS (http://earthexplorer.usgs.gov)
	NDVI	2015	30 m	NDVI is derived as the normalized ratio between surface reflectance of red band and near infrared band of Landsat images (Hwang et al., 2011)
Linear features and restricted area	Yangtze River, lakes;	2009-2012	30 m	A land-use map created by the Second National Land Survey in 2009
	Natural reserves, forest reserves;			Land Use Planning of Wuhan City 2009-2020
	Land for special uses			Forestry Department of Hubei Province 2010–2012
Socio-economic statistical data	Population, GDP;	2000-2015	NA	Wuhan Statistical Bureau 2001–2016 (www.stats-hb.gov.cn)
	Economic benefits and labor engaged in farming, forestry, animal husbandry and fishery;			National Agricultural Statistics (cost and income of agricultural products) 2016
	Production value of cropland			
Socio-economic spatial data	GDP density, Population density	2010	1 km	Interpolated grid data provided by RESDC (http://www.resdc.cn)
Physical condition	Silt, Sand, Clay contents;	1990s	1 km	Provided by RESDC (http://www.resdc.cn)
	Soil erosion;	1995	1 km	Provided by RESDC (http://www.resdc.cn)
	Elevation, Slope, Aspect;	2000s	90 m	DEM data are obtained from SRTM products by NASA (http://www.gscloud.cn). Slope and aspect are derived from DEM with ArcGIS
	Precipitation	Annual average	1 km	Interpolated grid data provided by RESDC (http://www.resdc.cn)
Spatial accessibility	Distance to residents	2009	30 m	The distribution of urban and rural residents, road, railway, airport, lakes, and rivers are extracted from the land-use map created by the Second National Land Survey.
	Distance to transportation nodes	2009	30 m	
	Distance to river and lake	2009	30 m	The distances to nearest residents, road, water, and city center are calculated in ArcGIS with the "Near" tool
	Distance to city center	2009	30 m	
Neighborhood effects	Neighborhood Effects of cropland, woodland, grassland, water area, built-up land and unused land	2015	30 m	The neighborhood effects are evaluated by the enrichment factor (Verburg et al., 2004) and calculated in ArcGIS with the "Focal statistics" and "Raster calculator" tools

The BAU scenario is generated from historical trends of land use changes, which represents a baseline without policy intervention. The RED and ELP scenarios are two optimized scenarios that subject to a set of constraints based on the needs for food, green space and urban development. The ultimate goal of the RED scenario is to maximize economic benefits derived from the land system, whereas the ELP scenario aims to protect ecosystems via land use planning and management.

BAU scenario: In the BAU scenario, the area of each land use type in 2030 is predicted by a GM (1, 1) grey model (Deng, 1989) based on historical land use data. Remotely sensed images in 2000, 2005, 2010 and 2015 are collected and classified, and linear interpolation is applied to generate continuous land use data from 2000 to 2015.

RED scenario: The objective of the RED scenario is to maximize the economic benefits provided by different land use types. The function of estimating economic benefits is expressed as Eq. (1):

$$f_1(x) = \sum_{i=1}^{6} Eco_i \cdot x_i \tag{1}$$

where $f_1(x)$ is the total economic benefits of all land use types, and x_i is the area for the i^{th} land use type. The index i represents a land use type ($n = 6$), and $i = 1, 2, \ldots, 6$ indicate cropland, woodland, grassland, water area, built-up land, and unused land, respectively; Eco_i is the economic benefits derived from per unit area of the i^{th} land use type. Gross output values of farming, forestry, animal husbandry and fishery are used to estimate the economic benefits obtained from cropland, woodland, grassland and water area, respectively. The gross domestic product (GDP) from the secondary and tertiary industry is derived as a proxy for the economic benefits of the built-up land. Based on the historical data from Wuhan Statistical Bureau (2001–2016) and the GM (1, 1) prediction, the Eco_i values (unit: 10^4 CNY/ha) of cropland, woodland, grassland, water area and built-up land are 6.70, 1.88, 198.04, 1.69, 1831.26, respectively. The Eco_i value of unused land is assumed to be zero. To derive comparable estimates throughout the time period, we convert the historical economic values to 2000constant market prices. Finally, Eq. (1) can be rewritten as:

$$f_1(x) = 6.70x_1 + 1.88x_2 + 198.04x_3 + 1.69x_4 + 1831.26x_5 + 0x_6 \tag{2}$$

Thus, the optimization function under the *RED scenario* is denoted as $max\ f_1(x)$.

ELP scenario: The objective of the ELP scenario is to maximize the ecological benefits provided by different land use types. We use ecosystem services value (ESV) and ecological capacity (EC) as the ecological functions to measure ecological benefits.

The function for ESV is expressed as Eq. (3):

$$f_2(x) = \sum_{i=1}^{6} Esv_i \cdot x_i \tag{3}$$

where $f_2(x)$ is the total ESV provided by the land system, Esv_i is the ESV of per unit area of i^{th} land use type (see section 3.3 for details). The total per-unit ESV of cropland, woodland, grassland, water area and unused land are 5.80, 20.63, 8.56, 33.27, and 1.02 (unit: 10^4 CNY/ha), respectively. The ESV of built-up land is set at zero, assuming no ecological benefits from built-up land (Costanza et al., 1997). Thus, the adjusted function for ESV can be expressed as Eq. (4):

$$f_2(x) = 5.80x_1 + 20.63x_2 + 8.56x_3 + 33.27x_4 + 0x_5 + 1.02x_6 \tag{4}$$

The function for EC is expressed as Eq. (5):

$$f_3(x) = \sum_{i=1}^{6} Ec_i \cdot x_i \times (100-12)\% \tag{5}$$

where $f_3(x)$ is the maximum EC provided by the land system, and $Ec_i = Q_i \times Y_i$ is the total EC of per unit area of ith land use type; Q_i is called the equivalence factor, which is calculated as the ratio of the biological productivity of the ith land use type to the global average

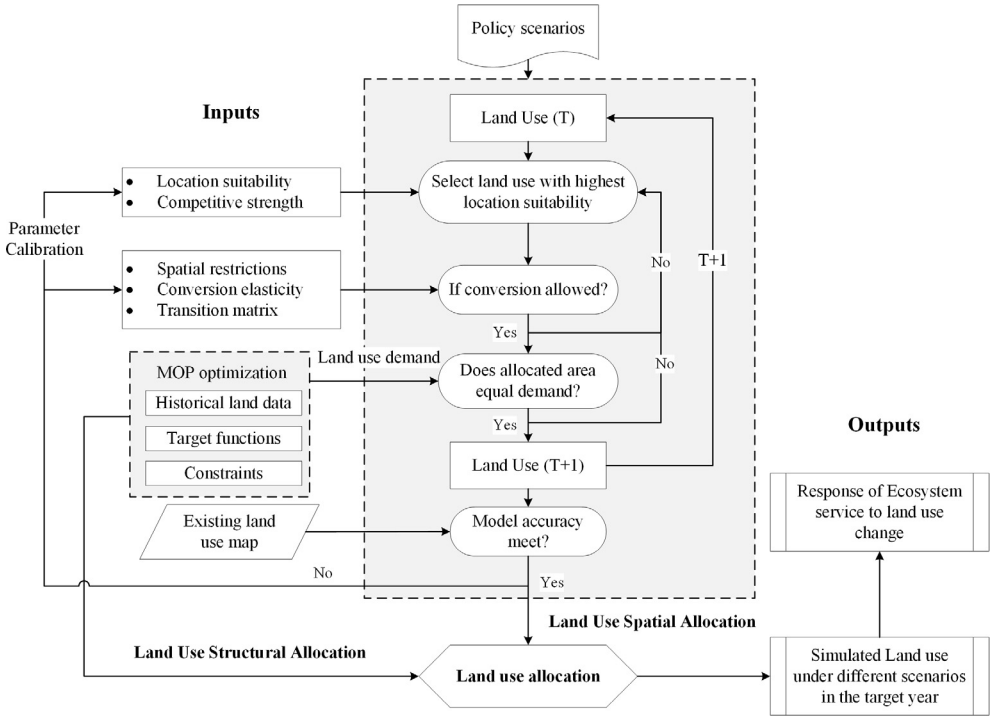

Fig. 2. Framework of the coupled model of MOP and Dyna-CLUE.

biological productivity of all bio-productive land use types; Y_i is called the yield factor, which is the ratio of local (i.e., Wuhan city) biological yield of the *i*th land use type to the global average biological yield of the same land use type (Li et al., 2010; Wang et al., 2014). The values for Q_i and Y_i are taken from our previous study (Wang et al., 2014). According to Wackernagel et al. (1999), 12% of the bio-productive land should be reserved for protecting biological diversity, and thus is deducted in the calculation of the EC. The adjusted function of EC can be expressed in Eq. (6):

$$f_3(x) = 5.00x_1 + 1.76x_2 + 0.08x_3 + 9.42x_4 + 2.50x_5 \quad (6)$$

Thus, the multi-objective optimization function under the *ELP scenario* is described as: *max* $\{f_2(x), f_3(x)\}$.

3.2.1.2 Constraints for RED and ELP scenarios. . The objective functions for optimization by the MOP algorithm subject to certain constraints based on empirical knowledge and existing city plans.

Constraint of the total land area: The sum of the area of each land use type should equal to the total area of Wuhan city, as written in the following equation:

$$\sum_{i=1}^{6} x_i = 845000 \quad (7)$$

Constraint of the total population: This constraint ensures that the total population living on land should not exceed the carrying capacity of land for human activity. According to "Wuhan City 2049 Strategic Development Plan" (CUPSD, 2014) and GM (1, 1) model, the total population of Wuhan city is projected to reach 14.2 million, and population densities on agricultural land (cropland, woodland, and grassland) and built-up land will be 0.55 and 48.93 persons per hectare by 2030, respectively. Therefore, the constraint for the total population can be written as:

$$0.55(x_1 + x_2 + x_3) + 48.93x_5 \leqslant 1.42 \times 10^7 \quad (8)$$

Constraint of landscape diversity: Grassland and unused land are frequently reclaimed for agricultural cultivation or urban development. The proportion of grassland and unused land in Wuhan city has declined from 1.71% to 1.50% during 2000-2015. To maintain the diversity of landscape as well as reserve space for urban development, we assume that at least one percent of the total land should be grassland and unused land by 2030. Thus, the constraint of land landscape diversity can be written as:

$$x_3 + x_6 \geqslant 1\% \times 845000 \quad (9)$$

Constraint of forest cover: The forest cover share is calculated based on "Ecological Green Equivalent", which refers to the "Green Amount" that can guarantee coequal photosynthesis and provide ecological functions of the quantitative forest. In the land system, land use types that satisfy the green equivalent include cropland, woodland and grassland, with coefficients of 0.46, 1.00 and 0.49, respectively, taken from the study by Liu et al. (2002). The proportion of forest cover in total land in Wuhan city is 28% in 2015 (WFB, 2016) and is expected to reach at least 30% of the total area by 2030. Therefore, the constraint of forest cover can be written as:

$$0.46x_1 + x_2 + 0.49x_3 \geqslant 30\% \times 845000 \quad (10)$$

Constraint of cropland area: The amount of grain produced by cropland (x_1), together with grain imported, should be equal to or larger than the demand of local population to secure food provision, which can be expressed as:

$$x_1 \cdot f_2 \cdot f_3 \cdot f_4 \geqslant P \cdot f_0 \cdot f_1 \quad (11)$$

where P is the predicted total population; f_0 is the amount of grain demand per capita, which is expected to reach 517.30 kg/capita by 2030 (Xin et al., 2015); f_1 is the grain self-sufficient rate (37.55%); f_2 is the grain yield per unit cropland area (6,312 kg/ha); f_3 is the rate of crop planting proportion (40.72%); f_4 is the multiple cropping index (2.85). The values of f_1 , f_2 , f_3 and f_4 are predicted by GM (1, 1) model based on historical data. Hence, a minimum of 376,825 ha of cropland (lower bound) will be needed to guarantee local self-sufficiency in food.

In addition, the cropland area has undergone a drastic decline from 61.06% to 53.00% from 2000 to 2015 mainly due to the expansion of built-up land. This conversion is unlikely to be reversed. Therefore, the upper bound of cropland area is the area of the status quo, i.e., cropland area in 2015. Therefore, the constraint of cropland area can be written

as:

$$376825 \leqslant x_1 \leqslant 447839 \quad (12)$$

Constraint of woodland area: The area of woodland in Wuhan city has declined from 78,261 ha to 75,096 ha during 2000-2015 and the decreasing trend is expected to continue. According to the "The 13th Five-Year Plan for Gardens and Forestry Development of Wuhan City (2016-2020)" (WFB, 2016) and the "Wuhan City 2049 Strategic Development Plan" (CUPSD, 2014), the local government is planning to implement more ecological protection programs. Hence, we set the area of 75,096 ha (i.e., the status quo) as the upper-bound value and the area of 64,001 ha (in 2030) predicted by historical data as the lower-bound value of woodland area, written as:

$$64001 \leqslant x_2 \leqslant 75096 \quad (13)$$

Constraint of grassland area: Since the 1990s, a substantial amount of grassland has been converted to built-up land and water bodies, leading to a decreasing trend. Here, we set 6,260 ha predicted by historical data as the upper bound for grassland in 2030, which can be written as:

$$0 \leqslant x_3 \leqslant 6260 \quad (14)$$

Constraint of water area: In the past few decades, large areas of water in Wuhan city have been reclaimed for urbanization and crop production. For instance, a large proportion of South Lake, Sha Lake, and South Taizi Lake are dominated by built-up land under construction (Wu, 2011). To prevent further shrinkage of lakes, the local government has carried out the "Three lines and One Road Protection Plan for Lakes in Central District" (WLRPB, 2012) for water conservation. Therefore, we assume that the decreasing trend of water area will slow down, and set the present area (173,125 ha) as the upper bound and the predicted area (165,132 ha) as the lower bound for water area, written as:

$$165132 \leqslant x_4 \leqslant 173125 \quad (15)$$

Constraint of built-up land area: Although the "Land Use Planning of Wuhan City (2006–2020)" (WLRPB, 2011) requires built-up land to be lower than 185,000 ha by 2020, we expect that the built-up land will exceed this limit after 2020 based the current growing trend. Meanwhile, the predicted area of built-up land is 267,203 ha in 2030. Thus, the area of built-up land will be between 185,000 ha and 267,203 ha in 2030, written as:

$$185000 \leqslant x_5 \leqslant 267203 \quad (16)$$

The constraint of unused land area: Since Wuhan has been reclaiming unused land for social-economic development, we expect a declining trend for the area of unused land. Therefore, the area of unused land in 2030 should be smaller than the present area of 5,682 ha in 2015, written as:

$$0 \leqslant x_6 \leqslant 5682 \quad (17)$$

3.2.2. Dyna-CLUE model: land use spatial allocation

We use the Dyna-CLUE model to allocate land use types in a spatially-explicit manner. The model runs iteratively and determines the most optimal land use type for each grid until the land demand predicted by the MOP algorithm for each scenario is satisfied.

3.2.2.1. Spatial policies and restrictions. Spatial policies and restrictions can directly influence land use spatial patterns through restricting certain land use changes in specific areas. Here, we specify three main spatial restrictions. First, the Yangtze River should not be converted to other land uses for all scenarios. Second, for the RED and ELP scenarios, six water reserves (Wu Lake, Chen Lake, Shangshe Lake, Cao Lake, Zhangdu Lake and Mulan Lake), two forest reserves (Jiufeng Mountain and Qinglong Mountain), several scenic spots and land for special uses (e.g., military, religion, and prison) are designated as spatial restrictions. Last, for the ELP scenario, the model also restricts the conversion of the 39 lakes protected by "Three lines and One Road Protection Plan for Lakes in Central District" (WLRPB, 2012) to other land use types.

3.2.2.2. Conversion settings. Conversion settings determine the change direction and the cost of conversion from one land use type to another. We specify two sets of parameters for each scenario, including the conversion elasticity (ELAS) and the conversion matrix.

The ELAS specifies the cost of conversions, with value ranges from 0 to 1. A higher value indicates higher converting cost, and thus a higher probability of irreversible change of a given location. A lower value, on the contrary, indicates lower cost to convert a land use type to another. In this paper, the ELAS values for model validation and BAU scenario design are determined by the total change rate of the transition matrix extracted from the land use maps during 2000-2015 (Table S2). Hence, the ELAS values are 0.76, 0.65, 0.34, 0.76, 0.86, and 0.34 for each land use type (Table S3). In addition, we adjust the values for RED and ELP according to other empirical studies (Hu et al., 2013; Zhang et al., 2015) and the specific context of each scenario.

The conversion matrix (x_{ik}) contains two values: value 1 indicates that all possible conversions may occur, while value 0 indicates that the conversion from the *i*th to the *k*th land use type is not allowed. The values are also extracted from the transition matrix (Table S2). The land use trend during 2000–2015 suggests that no conversions occur from cropland to grassland or unused land, from woodland to unused land, and from built-up land to grassland or unused land. Therefore, under the BAU scenario, the x_{ik} values for these conversions are set at 0, and others are set at 1. Under the other two scenarios, we assume that the conversions from cropland, woodland, and built-up land to unused land are not allowed. The detailed assumptions on all possible conversions under the BAU, RED, and ELP scenarios are listed in Table S4.

3.2.2.3. Location suitability analysis. The location suitability analysis evaluates the suitability of a location for a specific land use influenced by a range of biophysical and socioeconomic factors (Bürgi et al., 2005). Location suitability plays a dominant role in determining competitive capacities of different land use types at a specific location (Verburg et al., 2008). The potential factors that affect location suitability in this study are selected based on literature review and available data. We select twenty explanatory variables (Fig. 3) from four categories (Table 2): (*i*) physical condition, which includes elevation, slope, aspect, soil erosion, silt content, sand content, clay content, and precipitation; (*ii*) spatial accessibility, which includes distances to residence, river and lake, transport node (railways, roads, ports and airports), and city center; (*iii*) socioeconomic factors, including GDP and population; (*iv*) neighborhood effects of the six land use types. The neighborhood effect measures whether the occurrence of one land use type at a specific location positively or negatively correlates with the occurrence of the other land use types in neighboring grids. We use the enrichment factor by Verburg et al. (2004) to quantify the neighborhood effects, defined as:

$$F_{i,j,d} = \frac{n_{i,d,j}/n_{d,j}}{N_i/N} \quad (18)$$

where $F_{i,j,d}$ is the enrichment of neighborhood d of location j with the ith land use type; $n_{i,d,j}$ is the number of cells with the ith land use type in the neighborhood d of grid j; $n_{d,j}$ is the total number of cells in the neighborhood d; N_i is the total number of cells with the ith land use type and N is the total number of cells in the study area. We use a 5×5 rectangular window ($d = 2$) to cover the neighboring cells given a specific grid. The enrichment factors of cropland, woodland, grassland, water area, built-up land, and unused land are derived with the "Focal Statistics" tool in ArcGIS 10.3.

We use a logistic regression model to examine the suitability of a grid for a specific land use type influenced by the proposed factors (Verburg et al., 2002). The model is expressed as:

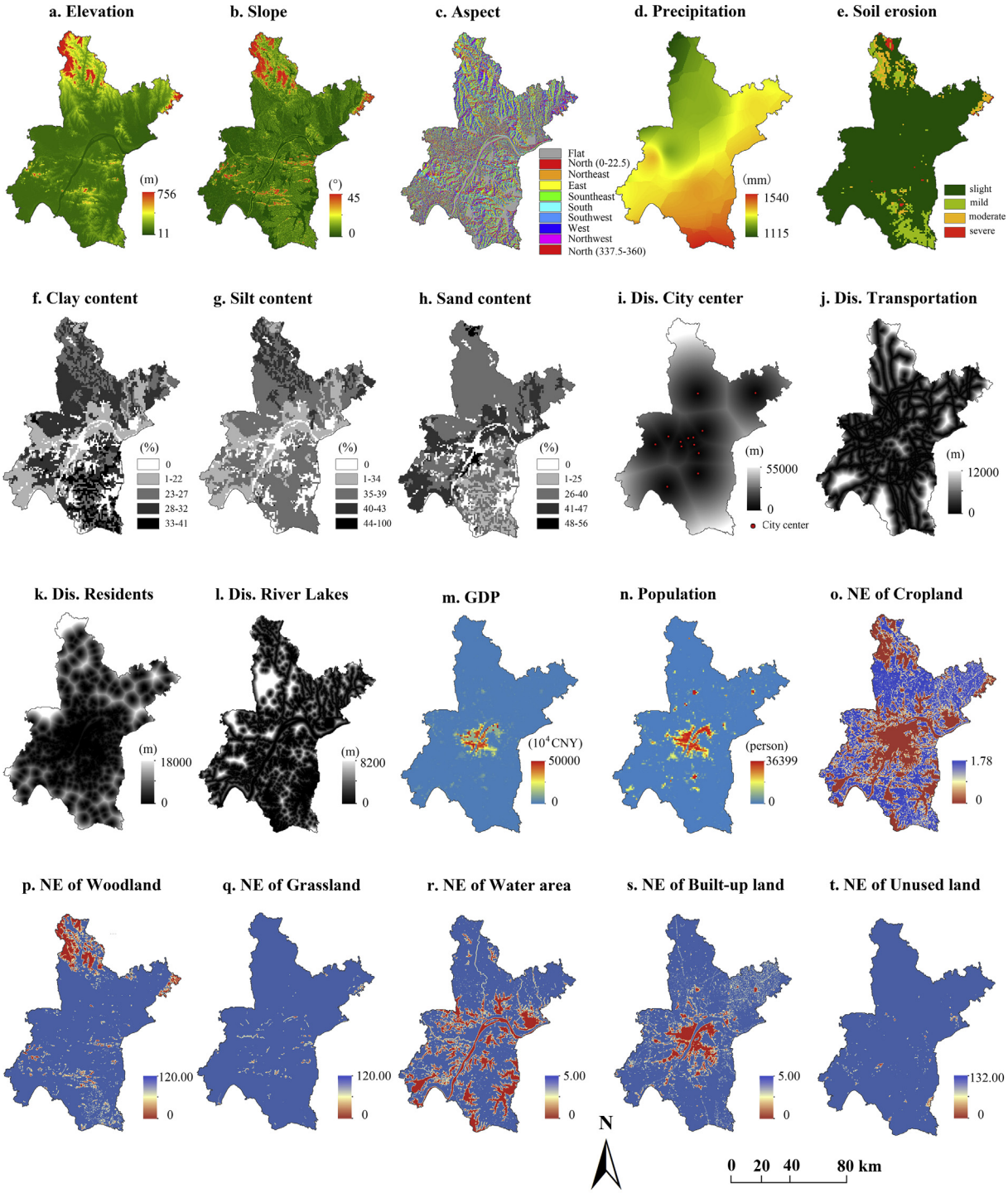

Fig. 3. Explanatory variables of location suitability in Wuhan City.

$$\mathrm{Log}\left(\frac{p(y_i=1)}{1-p(y_i=1)}\right)=\beta_0+\beta_1 m_1+\beta_2 m_2+\cdots+\beta_n m_n+\varepsilon \quad (19)$$

where $p(y_i = 1)$ is the probability of occurrence for the i^{th} land use type on a given grid; m_1, m_2, ..., m_n denote the explanatory variables; β_0 is the constant; β_1, β_2, ..., β_n are the regression coefficients; ε is the error term. The logistic regression model is applied for each land use type. We adopt the same estimated parameters for location suitability for all of the three scenarios.

Land use regression models often display the problem of spatial autocorrelation (Overmars et al., 2003). One method to handle this problem is spatial sampling that selects grids with sufficient distances between each grid (Cheng and Masser, 2003). The key to this method is to define a proper distance that can balance sample distribution with sample size so that the model can reduce spatial autocorrelation and meanwhile maintain robust estimation. Since the areas of grassland and unused land are relatively small, we choose a distance interval of 500 m for these two land use types, and 1500m for the others. For the sampling procedure, we use the "Convert" tool (Verburg and Overmars, 2009) to generate balanced samples for the dependent variable. Eventually, we obtain 3072, 569, 420, 1339, 1056, and 328 samples for cropland, woodland, grassland, water area, built-up land, and unused

Table 2
Logistic regression analysis of the spatial determinants of land use spatial occurrence.

Variables	Cropland	Woodland	Grassland	Water	Built-up	Unused
Physical condition						
Elevation (m_1)				−0.130***	−0.011†	−0.005
Slope (m_2)	−0.190***	0.749***	0.290***			
Aspect (m_3)	0.001**	0.006***	0.002†	−0.005***		0.004***
Soil erosion (m_4)	−0.116	−0.222		0.252	−0.438†	−0.620†
Silt content (m_5)			−0.016†			
Sand content (m_6)		−0.030*			0.017**	0.020*
Clay content (m_7)	0.056***	0.060**				
Precipitation (m_8)	2.33×10^{-4} ***	−0.001***		−0.001***		
Spatial accessibility						
Distance to residence (m_9)	0.134***			0.063	−0.322***	0.036
Distance to river and lake (m_{10})	0.474***	−0.113	−0.622***	−1.339***	0.140†	−0.972***
Distance to transport node (m_{11})	−0.064*	0.067	0.028	0.120*	−0.57***	0.538***
Distance to city center (m_{12})		0.084***	−0.055***	0.05***		
Socio-economic factors						
GDP (m_{13})		0.042	−0.037			
Population (m_{14})	−0.185***			−0.084*	0.314***	−0.024
Neighborhood effects (NE)						
NE of cropland (m_{15})		−0.866***		−0.311*	−0.049	
NE of woodland (m_{16})	−0.015		−0.034	0.020	−0.023	0.069
NE of grassland (m_{17})	−0.010†	−0.023	−0.007			
NE of water area (m_{18})	−0.084**	−0.228†	−0.033			0.204*
NE of built-up land (m_{19})	−0.034			−0.068†	0.019	−0.025
NE of unused land (m_{20})	−0.013**			−0.006		0.159†
Constant	−4.522***	8.009**	−1.831	15.749***	0.973**	−1.558**
Evaluation of performance						
AUC	0.760	0.955	0.785	0.887	0.850	0.836
0-correct percent	0.635	0.932	0.780	0.731	0.730	0.802
1-correct percent	0.760	0.848	0.701	0.851	0.786	0.718

*** $p < 0.001$.
** $p < 0.01$.
* $p < 0.05$.
† $p < 0.10$.

land, respectively. The ratio of samples for each binary dependent variable is nearly 1:1.

We also test multi-collinearity of the explanatory variables using a correlation matrix for each regression model (Table S5a–5f). After removing variables that are strongly correlated, we use variance inflation factors (VIF) and tolerance values to further test the multi-collinearity issue for each model (Table S6). The tests show that the VIF and tolerance values of all explanatory variables are less than 5 and greater than 0.2, respectively, suggesting little effects of multi-collinearity.

With estimated coefficients, we predict the probability of occurrence for each land use type (Table 2). We then use the probabilities of correct prediction and receiver operating characteristic (ROC) statistics to evaluate the goodness-of-fit of the regression models. The probabilities of correct prediction for all land use types range from 63.5% to 93.2% (Table 2), while the areas under ROC curve (AUC) range from 0.76 to 0.96 (Figure S1), suggesting that all of the models are reliable and adequate for future simulation.

3.2.3. Model validation

We use historical land use dataset from 2000 to 2015 to estimate regression coefficients and calibrate model parameters. The land use spatial distribution in year 2000 is regarded as a base map of the simulation, other inputs include the quantity of change for each land use type during 2000–2015 (extracted from historical land use maps), the conversion settings, the spatial restrictions, and the location suitability for each land use type on each grid. After running the Dyna-CLUE model for 15 years, the simulated land use map for 2015 can be obtained. Then, we evaluate the performance of the model by comparing the classified land use map in 2015 from a remote-sensed image in Wuhan city and the predicted map by the Dyna-CLUE model. The overall model accuracy is 74% under basic spatial restriction (Yangtze River is not allowed to convert to other land uses), indicating that the model parameter settings are acceptable and can be applied to predict future land use patterns. Hence, we use the validated parameters and the classified land use map in 2015 to project land use changes in 2030 under the three scenarios.

3.3. Ecosystem services valuation

To determine the potential impacts of land use changes on the provision of ES under the three scenarios, we adopt a proxy-based ES valuation method proposed by Costanza et al. (1997) and adapted by Xie et al., (2003, 2008). Costanza et al. (1997) grouped the global biosphere into 16 types of land cover (such as croplands, forest, wetlands) and 17 types of ES, and then estimated the per-unit value of each type of ES provided by each type of land cover (i.e., per-unit ESV coefficients). However, some problems emerge when directly applying the method for evaluating ecosystems in China. For example, some types of ES are not represented in Chinese ecosystems (Fu et al., 2016), and the per-unit ESV coefficients primarily estimated in developed countries may fail to reflect people's 'willingness-to-pay' for ES in developing countries like China, e.g., the ES provided by cropland may be less valued but the ES provided by wetlands are overvalued (Lin et al., 2013). Thus, Xie et al., (2003, 2008) proposed two major revisions of the model. First, they reclassified the ES into nine categories, including food production, raw materials, gas regulation, climate regulation, water regulation, waste treatment, soil maintenance, biodiversity protection and landscape aesthetics. Second, they modified the per-unit ESV coefficients of Costanza et al. (1997) and established the Chinese "equivalent value coefficients" table (Table S7) based on two surveys of 700 Chinese ecologists.

According to the ES valuation method, the economic value of food

Table 3
Projected land use areas and relative changes from 2015 to 2030 under BAU, RED, and ELP scenarios in Wuhan City.

LU type	Land use (ha)				Land use (%)				Relative change rate (%)		
	2015	BAU	RED	ELP	2015	BAU	RED	ELP	2015-BAU	2015-RED	2015-ELP
Ecological land[a]	703,041	573,987	627,621	657,782	83.20	67.93	74.27	77.84	−18.36	−10.73	−6.44
Cropland	447,839	338,641	381,160	403,827	53.00	40.08	45.11	47.79	−24.38	−14.89	−9.83
Woodland	75,096	63,978	75,088	74,585	8.89	7.57	8.89	8.83	−14.81	−0.01	−0.68
Grassland	6,981	6,247	6,247	6,242	0.83	0.74	0.74	0.74	−10.51	−10.51	−10.59
Water area	173,125	165,121	165,126	173,128	20.49	19.54	19.54	20.49	−4.62	−4.62	0.00
Built−up land	136,277	267,192	215,149	184,989	16.13	31.62	25.46	21.89	96.07	57.88	35.74
Unused land	5,682	3,821	2,230	2,229	0.67	0.45	0.26	0.26	−32.75	−60.75	−60.77

[a] The total area of ecological land is the sum of the areas of cropland, woodland, grassland, and water area.

production provided by cropland is defined as the standard value. The values of all other ES are converted into equivalent values corresponding to the standard value. The function of the conversion is expressed as:

$$VC_{ij} = D \times E_{ij} \tag{20}$$

where VC_{ij} is the per-unit value (CNY/ ha) of the jth ES provided by the ith land use type; E_{ij} is the equivalent value coefficient of the jth ES provided by the ith land use type in relation to food production of cropland (Table S7); D is the economic value of food production of per-unit cropland (i.e., the standard value). We calculate D based on agricultural data of Hubei Province (NDRC, 2016) to reflect the willingness-to-pay for ES of residents in Wuhan city. The agricultural data include cultivated areas and net income for subsistence crops in Hubei, including rice (early-, mid-, and late-season rice), wheat, and corn. The estimation of D is expressed as:

$$D = I_r P_r + I_w P_w + I_c P_c \tag{21}$$

where I_r, I_w and I_c are net income from grain production of rice, wheat and corn, respectively; P_r, P_w and P_c are the shares of cultivated areas for rice, wheat and corn, respectively. The estimated value for food production of per-unit cropland (i.e., D) is 2811.19 CNY/ ha in 2015.

To represent the spatial distribution of ESV, the valuation of ES in this study is conducted at the grid level (100 m × 100 m). Note that the land use type for each grid is predicted by the coupled land use change model as described above. Thus, the total ESV of a given grid is determined by adding up the values of all types of ES provided by the land use of the grid:

$$ESV_i = \sum_{j=1}^{9} a \times VC_{ij} \tag{22}$$

where ESV_i is the total ESV of a grid with ith land use type; a is the area of each grid and equals to 1 ha.

The valuation of ES at spatial scales needs to consider the spatial heterogeneity in ES provision of each land use type in different locations. Prior studies indicated that ES supply is positively associated with the amount of biomass covering the land (de Groot et al., 2002). The normalized difference vegetation index (NDVI) is widely used as an indicator of vegetated coverage and relative biomass (Calderón-Contreras and Quiroz-Rosas, 2017; Creech et al., 2016). Thus, we conduct a grid-by-grid modification based on NDVI for grids covered by cropland, woodland and grassland. The NDVI values for built-up land, water area, and unused are relatively low or negative, and thus are not considered. For a grid with the i^{th} land use type, the biomass modification coefficient (b_i) and the modified value (ESV_i') is defined as:

$$ESV_i' = \sum_{j=1}^{9} a \times VC_{ij} \times b_i \tag{23}$$

$$b_i = \frac{NDVI_i}{NDVI_{i,max}} \tag{24}$$

where $NDVI_i$ is the NDVI value for grids with the ith land use type, and $NDVI_{i,max}$ is the maximum NDVI value of the ith land use type among all grids.

Eventually, the total ESV of Wuhan city is the sum of the ESV_i' values of all grids.

4. Results

4.1. Projected land use changes during 2015–2030

The impacts of spatial determinants on the spatial occurrence of each land use type is estimated by the logistic regression model (Table 2). Both cropland and built-up land compete for areas with lower soil erosion risks, better access to transport nodes, longer distances to water, and in the vicinity to woodland. In addition, the occurrence of cropland is also positively associated with precipitation, but negatively with slope and population. Built-up land is more likely to occur in areas with lower altitudes, closer to residence, and higher population density. Woodland tends to occur in remote areas with higher slopes and longer distances to city center.

Table 3 shows the predicted area and relative change of each land use type under the three scenarios. In 2015, the cropland accounted for the lion's share (53%) of the total land area in Wuhan city, followed by water area (20%) and built-up land (16%), while the area of woodland was modest (9%). The coupled land use model predicts substantial growths in built-up land between 2015 and 2030 under all of the three scenarios. As expected, the BAU scenario presents the highest rate of built-up land expansion (a 96% increase relative to 2015), which is much higher than those under RED and ELP, with expansion rates of 58% and 36%, respectively. The increase in built-up land occurs at the expense of all other land use types. Particularly, cropland experiences the greatest area loss across all scenarios. Comparing the projections for the BAU and ELP scenarios clearly demonstrates the importance of land use planning and other regulations in protecting ecological lands. For example, under ELP, the woodland and water area remain stable and cropland shrinks at a lower rate, but unused land and grassland have larger declines than under BAU.

Land use conversion matrix is also provided to reveal the major land use transitions during the simulation period (Table 4). Under BAU, we can see fewer pairs of conversions in the land system, with most of these conversions going from other land use types to built-up land. In contrast, the two optimized scenarios (i.e., RED and ELP) present more conversions among cropland, woodland, grassland, water area and unused land, leading to both losses and gains in these land use types. Instead, built-up land is rather stable with the total conversions to other land use types being smaller than 1.2% under all scenarios.

Fig. 4 shows the predicted land use maps in 2030 and the changes from 2015 to 2030 of the four dominant land use types under the three scenarios. The built-up land is concentrated in the center of Wuhan city and occupies a considerable part of the total area, especially under the BAU scenario. Cropland and lakes locate at the periphery of built-up

Table 4
Land use conversion matrix from 2015 to 2030 under BAU, RED, and ELP scenarios in Wuhan City (%).

Scenarios	From 2015 to 2030	Cropland	Woodland	Grassland	Water area	Built-up land	Unused land
BAU	Cropland	75.61	0.71		0.62	23.06	
	Woodland	0.03	80.35	3.30	0.79	15.5	0.04
	Grassland		1.63	49.99	2.86	42.6	2.91
	Water area			0.05	93.09	6.86	
	Built-up land		0.13		0.14	99.73	
	Unused-land		3.29	3.22	3.36	27.00	63.13
RED	Cropland	84.97	1.10	0.18		13.75	
	Woodland	0.28	90.89	0.49	0.05	8.27	0.02
	Grassland	0.09	6.09	62.23	0.60	30.58	0.42
	Water area	0.05	0.41	0.04	95.2	4.31	
	Built-up land	0.03	0.13	0.06		99.78	
	Unused-land	5.51	10.45	10.08	4.26	31.19	38.51
ELP	Cropland	89.92	0.22	0.13	0.05	9.68	
	Woodland	0.01	96.5		0.03	3.45	
	Grassland	0.49	2.08	78.57	1.30	16.67	0.89
	Water area	0.03	0.02	0.01	99.11	0.81	0.01
	Built-up land	0.48	0.41	0.10	0.18	98.84	
	Unused-land	6.48	7.16	0.48	16.9	31.29	37.7

areas, while woodland is highly concentrated and mainly distributed in the northwest part of the city. The shrinkages of cropland are spatially consistent with the gains of built-up land, confirming that urban expansion in Wuhan city encroaches cropland, mostly along transport lines, near residential areas and city centers, which is consistent with the findings in the regression model (Table 2) and other empirical

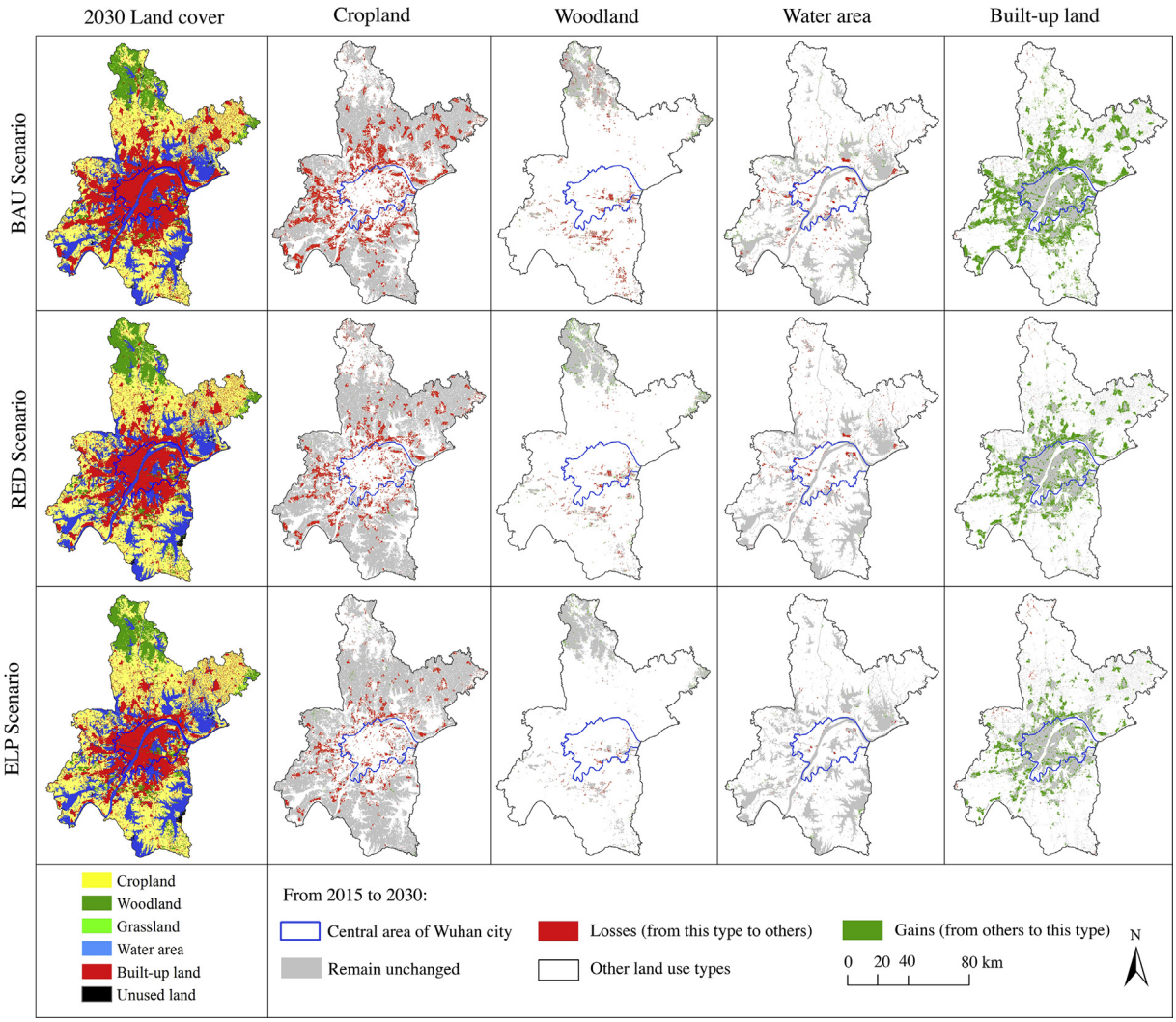

Fig. 4. Spatial patterns of land cover in 2030 and changes between 2015 and 2030 under BAU, RED, and ELP scenarios, for cropland, woodland, water area and built-up land.

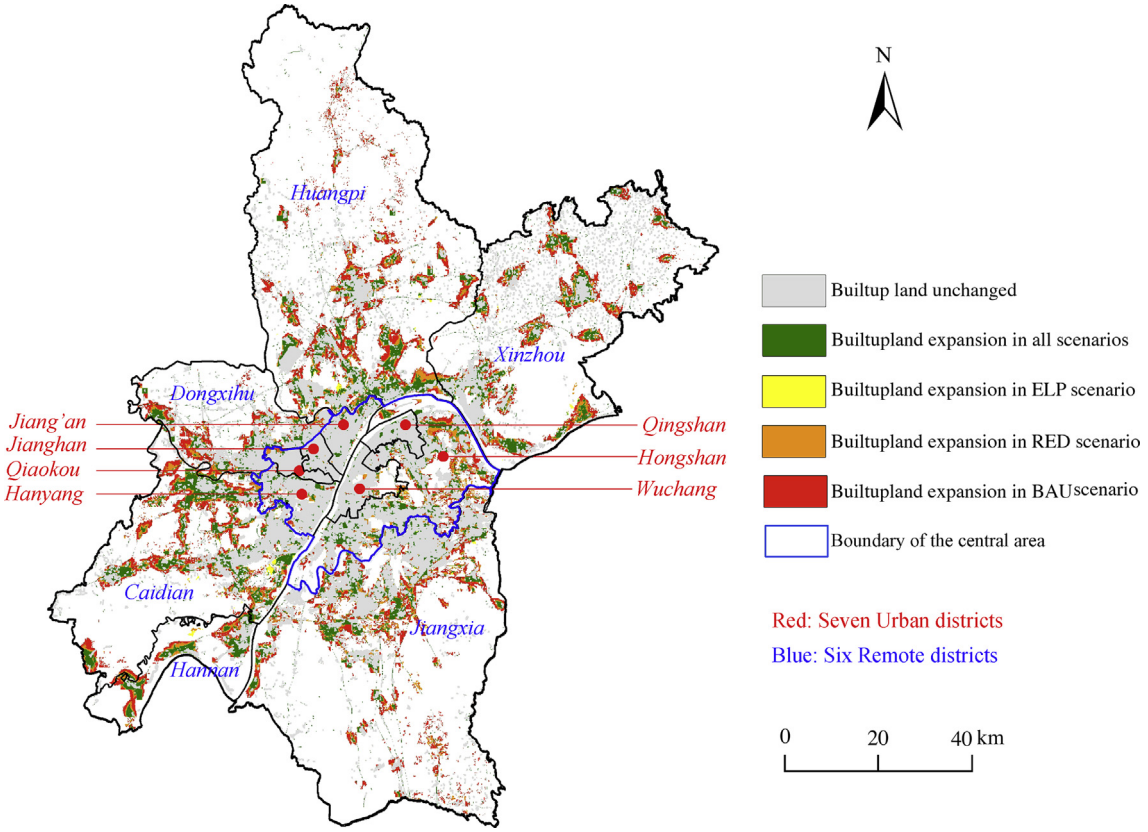

Fig. 5. Hotspots for built-up land expansion.

studies (Marcotullio and Lee, 2003; Mathur, 2005).

We also conduct a spatial analysis to identify the "hotspots" of urban expansion by extracting the overlapping areas of built-up land gains under all of the three scenarios. Most land in the seven urban districts has already been developed for built-up uses by 2015, except for Hongshan district, which still has some hotspots of urban expansion in the eastern part during 2015–2030. As shown in Fig. 5, most of the hotspots are located in the six remote districts, which suggests that these areas would experience rapid urbanization during 2015–2030. By 2030, the most remarkable urban sprawl would occur in Caidian district, followed by Huangpi, while Jiangxia and Dongxihu would have relatively smaller urban area growths. Built-up land of Huangpi mainly extends south towards the central area of Wuhan city or expands along the boundary of the central area, rather than around the center of Huangpi district. In contrast, built-up areas in Jiangxia and Caidian expand in the opposite direction of the central area. New built-up land tends to occur on the fringes of existing urban and rural residence. The hotspots of Xinzhou and Hannan districts are more scattered than other districts.

4.2. Variations in ecosystem service value during 2000–2030

Table 5 presents the variations in total ESV and individual ESV for each land use type during 2000–2015, and the predicted ESV in 2030 under the three scenarios. Water regulation and waste treatment are the two dominant types of ES in Wuhan city, which accounted for 29% and 25% of the total ESV in 2015, respectively. In contrast, food production (4%) and raw material provision (3%) accounted for the smallest parts. From 2000 to 2015, the total ESV in Wuhan city decreased by 3.63%, and meanwhile, each individual ESV also declines. Specifically, food production and soil maintenance experienced the greatest losses, while water regulation and landscape aesthetics services remained stable. This decreasing trend continues in the period of 2015–2030 for all scenarios. Not surprisingly, the BAU scenario presents the greatest loss of the total ESV with a relative decrease of 10.83%, followed by RED (decrease by 6.04%) and ELP (decrease by 2.34%). Similarly, each individual ESV declines under all of the three scenarios. The shrinkages of the total ESV and individual ESV demonstrate that the ongoing urban sprawl in Wuhan city has profound negative impacts on ecosystems.

The spatial distributions of the total ESV of Wuhan city in 2030 under BAU, RED, and ELP scenarios are shown in Fig. 6A–C. The central area and its surrounding areas where the landscape is dominated by built-up land exhibit the lowest ESV. Areas with moderate ESV are mainly located in the six remote districts, which is spatially consistent with the distributions of cropland and grassland. The northern region covered by forest and the areas covered by water surfaces represent the highest ESV. Fig. 6D–F provides spatially-explicit information on the gains and losses of ESV during 2015–2030 under alternative scenarios. As expected, the BAU scenario is associated with greater ESV losses both within and around the central area, compared with the other two scenarios. The areas that present the largest ESV declines are caused by the conversion of water bodies (e.g., ponds and lakes) to urban land. The ESV gains primarily occur in remote areas, e.g., the northeastern corner in Xinzhou district and the northern area in Huangpi district. These gains are contributed by the transition from cropland to woodland.

4.3. Interactions between land uses and ecosystem services

To quantify how interactions between land use types bring about trade-offs among multiple ES, we establish the ESV change matrix (Table 6) based on the equivalent coefficients table (Table S7). It summarizes ESV trade-offs driven by unit area (1 ha) land use transitions. For example, the conversion from cropland to water area can lead to trade-offs among the provision of multiple ES, i.e., a group of services (e.g., food production, raw material, gas regulation and soil

Table 5
Variations in ecosystem service value during 2000–2030.

Ecosystem services	ESV (10^9 CNY)					ESV relative changes (%)			
	2000	2015	BAU	RED	ELP	2000–2015	2015-BAU	2015-RED	2015-ELP
Food production	1.79	1.60	1.28	1.41	1.48	−10.68	−19.60	−11.60	−7.02
Raw material	1.40	1.30	1.09	1.23	1.26	−7.08	−15.88	−4.94	−3.29
Gas regulation	2.27	2.10	1.75	1.98	2.02	−7.64	−16.47	−5.80	−3.85
Climate regulation	3.32	3.12	2.67	2.91	3.01	−6.26	−14.33	−6.47	−3.51
Water regulation	11.05	11.00	10.23	10.46	10.91	−0.42	−6.95	−4.93	−0.78
Waste treatment	9.54	9.37	8.58	8.80	9.21	−1.82	−8.43	−6.11	−1.68
Soil maintenance	3.26	2.95	2.39	2.69	2.78	−9.68	−18.83	−8.59	−5.66
Biodiversity protection	4.16	3.95	3.44	3.71	3.83	−5.11	−12.82	−6.14	−2.98
Landscape aesthetics	2.85	2.83	2.62	2.71	2.81	−0.69	−7.43	−4.39	−0.75
Total	39.64	38.20	34.07	35.90	37.31	−3.63	−10.83	−6.04	−2.34

maintenance services) are “traded off” to enhance the provision of another group of services (e.g., climate regulation, water regulation, waste treatment, biodiversity protection, and landscape aesthetics). In contrast, the conversion from cropland to built-up land leads to net loss of all individual services, as the ES provided by built-up land is considered as zero. Combined with land use transition matrix from 2015 to 2030 (Table 4), the detailed ESV change for all predicted land use transitions for the three scenarios can be estimated (Table S8a–c).

Here, we present the major land use transitions that are projected by our coupled land use model during 2015-2030, and the associated trade-offs among multiple ES. The transition from cropland to built-up land, which dominates land use changes in Wuhan city, leads to the largest ESV loss in total ESV, i.e., 2293, 1368 and 963 million CNY under BAU, RED, and ELP, respectively (Table S8a–c). Specifically, values of soil maintenance, waste treatment and food production services are expected to decline to the greatest extent, primarily driven by the conversion from cropland to built-up land.

Built-up land expansion at the loss of water area has stronger negative impacts on ecosystems, and triggers greater loss of ESV. The BAU scenario exhibits the highest conversion from water area to built-up land (6.86%) (Table 4), which leads to a net loss of 1514 million CNY in total ESV (Table S8a) while the ES loss driven by this conversion under ELP is only 179 million CNY (Table S8c). This is because the most strict spatial regulations are involved in ELP to forbid the conversion of the Yangtze River and the 39 lakes to other uses, according to the “Three lines and One Road Protection Plan for Lakes in Central District”. Thus only 0.81% of the total water area would be occupied by urban sprawl under ELP (Table 4). The conversion from water bodies to built-up areas leads to the greatest loss of water regulation and waste treatment services. Forests have played important roles in local and regional biodiversity protection, climate regulation, and gas regulation (Turner et al., 2014). Thus, the conversion from woodland to built-up land is associated with substantial loss in the provision of these services (Table 6).

5. Discussions

5.1. The coupled model: a useful tool for land use planning

Establishing optimized land use schemes is a fundamental task of

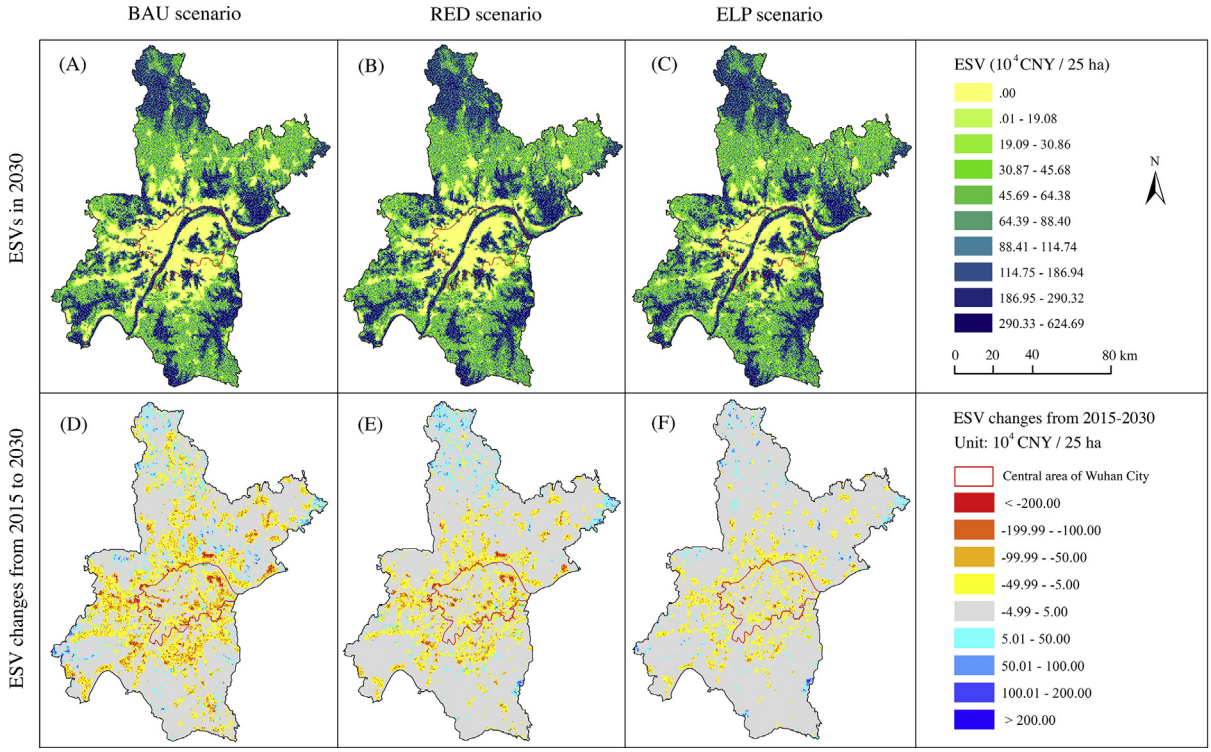

Fig. 6. Spatial patterns of ESVs in 2030 (500 m × 500 m cells) under BAU scenario (A), RED scenario (B), ELP scenario (C), and changes between 2015 and 2030 under BAU scenario (D), RED scenario (E), and ELP scenario (F).

Table 6
Ecosystem service change matrix driven by per-unit LU land-use transitions, unit: CNY/(ha year).

Land use transition From	To	Total ES changes	Food production	Raw material	Gas regulation	Climate regulation	Water regulation	Waste treatment	Soil maintenance	Biodiversity protection	Landscape aesthetics
Cropland	Woodland	56842	−1883	7281	10120	8715	9333	928	7169	9811	5369
	Grassland	10598	−1602	−84	2193	1659	2108	−197	2165	2390	1968
	Water area	105279	−1321	−112	−590	3064	50601	37839	−2980	6775	12004
	Built−up	−22208	−2811	−1096	−2024	−2727	−2165	−3908	−4132	−2867	−478
	Unused land	−18301	−2755	−984	−1855	−2361	−1968	−3177	−3655	−1743	197
Woodland	Cropland	−56842	1883	−7281	−10120	−8715	−9333	−928	−7169	−9811	−5369
	Grassland	−46244	281	−7365	−7928	−7056	−7225	−1124	−5004	−7422	−3402
	Water area	48437	562	−7393	−10711	−5650	41268	36911	−10148	−3036	6634
	Built−up	−79051	−928	−8377	−12144	−11442	−11498	−4835	−11301	−12678	−5847
	Unused land	−75143	−871	−8265	−11976	−11076	−11301	−4104	−10823	−11554	−5173
Grassland	Cropland	−10598	1602	84	−2193	−1659	−2108	197	−2165	−2390	−1968
	Woodland	46244	−281	7365	7928	7056	7225	1124	5004	7422	3402
	Water area	94681	281	−28	−2783	1406	48493	38035	−5144	4385	10036
	Built-up land	−32807	−1209	−1012	−4217	−4385	−4273	−3711	−6297	−5257	−2446
	Unused land	−28899	−1153	−900	−4048	−4020	−4076	−2980	−5819	−4132	−1771
Water area	Cropland	−105279	1321	112	590	−3064	−50601	−37839	2980	−6775	−12004
	Woodland	−48437	−562	7393	10711	5650	−41268	−36911	10148	3036	−6634
	Grassland	−94681	−281	28	2783	−1406	−48493	−38035	5144	−4385	−10036
	Built-up	−127487	−1490	−984	−1434	−5791	−52766	−41746	−1153	−9642	−12482
	Unused land	−123580	−1434	−871	−1265	−5426	−52569	−41015	−675	−8518	−11807

Note: Developed based on the equivalent coefficients table for ecosystem service value per unit area of each land use type in China, source: Xie et al (2008).

land use planning, which involves the allocation of land resources to meet the demands of different economic sectors. However, traditional land use structure optimization approaches adopted by previous land use planning are not efficient in allocating the predicted land demands to the most suitable locations. The coupled model developed in this study integrates the MOP algorithm and the Dyna-CLUE model to simultaneously optimize land use quantitative structure and spatial pattern from the top-down and bottom-up perspectives. First, the MOP algorithm predicts optimized land use demands with the aim of maximizing economic or ecological objectives specified by different scenarios subject to a set of socioeconomic and ecological constraints. The top-down process represents the land use decision-making at the macro-level (e.g., country, province and local government) by making use of land resources to achieve specific purposes according to policy designation. Then, the Dyna-CLUE model enables not only the allocation of the projected land use demands to the most suitable locations, but also the involvement of spatial development and restriction policies following a bottom-up process. The coupled model can be applied in land use planning to assist the design of land use optimization schemes concerning both quantitative structure and spatial pattern. In addition, it can be extended by incorporating scenario analysis and ecological modeling, which allows managers to predict future land use changes and possible effects on multiple ES, and ultimately lead to more informed policy design and implementation.

5.2. Trade-off analysis: a possible way to balance intended and unintended ecosystem outcomes

Land management choices that enhance intended ES are often accompanied by unintended (often negative) ecosystem outcomes (Defries et al., 2004). These outcomes may not occur at locations where the decisions are made and involve time-lags, and thus are often neglected by policy-makers and natural-resource managers. Therefore, the first but critical step towards sustainable management of ecosystems is to raise their awareness about the potential ES trade-offs that arise from their decisions. To achieve this goal, we establish an ESV change matrix (Table 6) that links each pair of land use transition with its associated gains and losses among multiple types of ES. The matrix reveals that the conversions between ecological land use types can trigger ES trade-offs (i.e., enhance the provision of some but at the expense of others), but the conversion from ecological lands towards a built-up use leads to net loss of all types of ES. Since land use transitions in our study area are dominated by the conversion from ecological lands to built-up land, all individual ES present decreasing trends, indicating net losses of multiple ES due to urban expansion. We have not found other complex interrelations of ES arise from land use changes, such as synergies, trade-offs, win-no change, lose-no change and no change, as found in other empirical studies (Haase et al., 2012; Turner et al., 2014). However, both this study and other studies on ES trade-offs have confirmed the potential role of trade-off analysis in land use planning and other environment policy making. It allows policy-makers to gain a comprehensive understanding of the potential effects of their decisions on ES trade-offs (Rodríguez et al., 2006), and seek a balance between intended and unintended ecosystem consequences (Defries et al., 2004). In addition, although the ecological benefits provided by built-up land can be neglected (Costanza et al., 1997), its socioeconomic benefits are huge. In many developing countries, economic benefits are the primary consideration in land resources management while the ecological benefits are often traded off, which may impose accumulative pressure on natural ecosystems and threatens regional ecological security. Thus, trade-off analysis also offers a method for policy-makers to make sound decisions that balance the socioeconomic and ecological benefits.

5.3. Policy implications

In this study, we choose Wuhan city as our study area, because it is a typical representative of the rapid urbanization areas in China that witness extensive built-up land expansions at the expense of ecological lands, which have led to great losses of high-quality cropland, irreversible damages in the city's water systems (both qualitatively and quantitatively) (Du et al., 2010), and frequent episodes of heavy haze (Lu et al., 2017). To restore the degraded ecosystems, the local government initiated several new ecological protection plans, including the "13th Five-Year Plan for Gardens and Forestry Development of Wuhan

City (2016–2020)", the "Three lines and One Road Protection Plan for Lakes in Central District", and the "Wuhan City 2049 Strategic Development Plan". Due to its advantageous location, Wuhan City is identified as a new economic growth engine of China by the "Development Plan for City Clusters along the Middle Reaches" in 2015 (China State Council, 2015). Therefore, Wuhan City has a high development potential and is currently at an accelerating stage of urbanization, which will impose a greater challenge to the sustainable provision of ES. Projecting future land use changes and their possible impacts on ES under different development scenarios is useful for responding to the challenge.

Thus, we design two optimized land use schemes for Wuhan city in 2030 by integrating the new ecological protection plans, with one maximizing economic benefits (i.e., the RED scenario) and the other maximizing ecosystem benefits (i.e., the ELP scenario). We also predict land use structure in 2030 based on historical land use trends (i.e., the BAU scenario), to which the two schemes of interest can be compared. As a result, the rapid and extensive built-up expansion is effectively controlled under either RED or ELP, with less ecological land being converted to urban uses during 2015-2030, compared to BAU (Table 3). More importantly, the two optimized land use schemes are more sustainable and resilient, because they take into account the land needed for "feeding" and "holding" the growing urban and rural population in 2030 predicted by the "Wuhan City 2049 Strategic Development Plan". The areas of woodland, grassland, and water bodies also satisfy the demands of related forest and water resources protection plans. The six water reserves, two forest reserves, and several major scenic spots in Wuhan city are protected from being converted to other uses under both RED and ELP. We also successfully introduce the "Three lines and One Road Protection Plan for Lakes in Central District" into the design of spatial restrictions of the ELP scenario to protect major city lakes from encroachment by urban expansion. A comparison between the two optimized scenarios shows more ecological lands are converted to urban uses under RED to yield economic prosperity, while the ELP scenario is more efficient in protecting water area and cropland, which may contribute to building a more ecologically-friendly city. Consequently, the land use changes under the ELP scenario has the smallest negative impacts on ecosystems with the total ESV decreasing by 2.34% relative to 2015, whereas the relative shrinkages under RED and BAU are 6.04% and 10.83%, respectively. Although the two optimized land use schemes fail to reverse the declining trends in ESV, they present much smaller losses of ES than the BAU scenario. This suggests the Wuhan city should reinforce the implementation of the natural resources protection plans and spatial regulations, which can effectively mitigate ecosystem degradation.

We also identify the "hotspots" of urban expansion in Wuhan city, which are locations that would experience the conversion from cropland to built-up land as predicted by all of the three scenarios, and thus are most likely to see urban sprawl at the loss of cropland than other areas. Therefore, land use spatial regulations should be executed to prevent the potential disorderly urban expansion in these hotspots and prohibit the occupation of high-quality cropland. The hotspots analysis also indicates most land use changes in the following decade will take place in Hongshan district (in the central area) and the six remote districts. Owing to differences in geographic, natural, and socioeconomic conditions, these districts exhibit different built-up expansion modes, such as the "infilling" mode in Hongshan, the "edge expanding" mode in Huangpi and Jiangxia, and the "leapfrogging" mode in Xinzhou and Hannan. Thus, diversified land management strategies are needed to guide the allocation of local land and other resources (such as tourism and cultural resources) in different districts to achieve both socioeconomic and ecological benefits. Moreover, these districts should adopt more efficient use of existing built-up areas, such as redeveloping shanty towns, "villages inside city", and discarded factories, as suggested by Liu et al. (2015b). In contrast, the "pancake-shaped" mode of urban sprawl in the central area of Wuhan city and other metropolises (e.g., Wang et al., 2007) that encroaches high-quality cropland and green space should be avoided.

In this study, we adopt the proxy-based ES valuation method proposed by Costanza et al. (1997) and set the ESV of built-up land at zero. However, some built-up land may provide recreation or cultural services, while some others have negative ecosystem outcomes, which could be considered as having negative ESV (Liu et al., 2012). Hence, our future work will involve the evaluation of ESV of built-up land, the design of optimized land use schemes that balance socioeconomic and ecological benefits, and the associated trade-offs driven by land use changes at a larger temporal scale.

6. Conclusions

In this study, we explore how land use changes under different development scenarios will affect the provision of ecosystem services (ES) in a megalopolis (i.e., Wuhan city) facing intensified land use conflicts. First, we design a coupled model that integrates the Multi-Objective Programming (MOP) and the Dynamic Conversion of Land Use and its Effects (Dyna-CLUE) models to project land use changes to the year of 2030 for Wuhan city under three scenarios: Business As Usual (BAU), Rapid Economic Development (RED), and Ecological Land Protection (ELP). Then, we adopt a proxy-based ES valuation method to predict the potential impacts of land use changes on the provision of ES under the three scenarios. We find that (1) the predicted land use changes during 2015-2030 are dominated by land use transitions from ecological lands (including cropland, woodland, grassland land, and water body) to built-up land. The annual expanding speed of built-up area under the three scenarios shows the following sequences, BAU (6.4%) > RED (3.9%) > ELP (2.4%). (2) The spatial pattern of built-up land growth is consistent with the shrinkage in cropland, which is projected to be the greatest near major residential areas and along transport lines. (3) The projected land use changes during 2015-2030 would lead to declines in the provision of ES under all scenarios, but the optimized land use scheme under ELP present the smallest loss of ES. This suggests the implementation of natural resources protection policies (e.g., forest and lake protection plans) and spatial restrictions (e.g., forbid changes in natural reserves) can effectively mitigate ecosystem degradation. (4) The ES value change matrix proposed in this work establishes the linkage between land use changes and ES trade-offs, which could be used as a policy tool to assess potential effects of land management choices, and guide the design of more informed decisions.

Acknowledgements

This research is funded by the National Natural Science Foundation of China (41501183), the Fundamental Research Funds for the Central Universities, China Unversity of Geosciences (Wuhan) and the China Scholarship Council. Also, the authors are grateful to the Data Center for Resources and Environmental Sciences, Chinese Academy of Sciences (RESDC) (http://www.resdc.cn) and the International Scientific & Technical Data Mirror Site, Computer Network Information Center, Chinese Academy of Sciences (http://www.gscloud.cn) for the access to the spatial data. We are also grateful to the anonymous reviewers for their invaluable and constructive comments that help us improve the manuscript.

Appendix A. Supplementary data

Supplementary data associated with this article can be found, in the online version, at https://doi.org/10.1016/j.ecolind.2018.06.047.

References

Azadi, H., Barati, A.A., Rafiaani, P., Taheri, F., Gebrehiwot, K., Witlox, F., Lebailly, P.,

2017. Evolution of land use-change modeling: routes of different schools of knowledge. Landsc. Ecol. Eng. 13, 319–332. https://doi.org/10.1007/s11355-016-0311-9.
Birch, J.C., Newton, A.C., Aquino, C.A., Cantarello, E., Echeverria, C., Kitzberger, T., Schiappacasse, I., Garavito, N.T., 2010. Cost-effectiveness of dryland forest restoration evaluated by spatial analysis of ecosystem services. Proc. Natl. Acad. Sci. 107, 21925–21930.
Bürgi, M., Hersperger, A.M., Schneeberger, N., 2005. Driving forces of landscape change – current and new directions. Landsc. Ecol. 19, 857–868. https://doi.org/10.1007/s10980-005-0245-3.
Calderón-Contreras, R., Quiroz-Rosas, L.E., 2017. Analysing scale, quality and diversity of green infrastructure and the provision of Urban ecosystem services: a case from Mexico City. Ecosyst. Serv. 23, 127–137.
Cheng, J., Masser, I., 2003. Urban growth pattern modeling: a case study of Wuhan city. PR China 62, 199–217.
China State Council, 2015. Development Plan for City Clusters along the Middle Reaches.
Chinese Institute of Urban Scientific Planning and Design (CUSPD), 2014. Wuhan City 2049 Strategic Development Plan.
Chuai, X., Huang, X., Lai, L., Wang, W., Peng, J., Zhao, R., 2013. Land use structure optimization based on carbon storage in several regional terrestrial ecosystems across China. Environ. Sci. Policy 25, 50–61. https://doi.org/10.1016/j.envsci.2012.05.005.
Clough, Y., Krishna, V.V., Corre, M.D., Darras, K., Denmead, L.H., Meijide, A., Moser, S., Musshoff, O., Steinebach, S., Veldkamp, E., Allen, K., Barnes, A.D., Breidenbach, N., Brose, U., Buchori, D., Daniel, R., Finkeldey, R., Harahap, I., Hertel, D., Holtkamp, A.M., Hörandl, E., Irawan, B., Jaya, I.N.S., Jochum, M., Klarner, B., Knohl, A., Kotowska, M.M., Krashevska, V., Kreft, H., Kurniawan, S., Leuschner, C., Maraun, M., Melati, D.N., Opfermann, N., Pérez-Cruzado, C., Prabowo, W.E., Rembold, K., Rizali, A., Rubiana, R., Schneider, D., Tjitrosoedirdjo, S.S., Tjoa, A., Tscharntke, T., Scheu, S., 2016. Land-use choices follow profitability at the expense of ecological functions in Indonesian smallholder landscapes. Nat. Commun. 7, 13137.
Costanza, R., D'Arge, R., De Groot, R.S., Farber, S., Grasso, M., Hannon, B., Limburg, K., Naeem, S., O'Neill, R.V., Paruelo, J., 1997. The value of the world's ecosystem services and natural capital. Nature 387, 253–260.
Costanza, R., de Groot, R.S., Sutton, P., van der Ploeg, S., Anderson, S.J., Kubiszewski, I., Farber, S., Turner, R.K., 2014. Changes in the global value of ecosystem services. Glob. Environ. Chang. 26, 152–158. https://doi.org/10.1016/j.gloenvcha.2014.04.002.
Creech, T.G., Epps, C.W., Monello, R.J., Wehausen, J.D., 2016. Predicting diet quality and genetic diversity of a desert-adapted ungulate with NDVI. J. Arid Environ. 127, 160–170.
Daily, G.C., Alexander, S., Ehrlich, P.R., Goulder, L., Lubchenco, J., Matson, P.A., Mooney, H.A., Postel, S., Schneider, S.H., Tilman, D., Woodwell, G.M., 1997. Ecosystem services: benefits supplied to human societies by natural ecosystems. Issues Ecol. 1–16 1092-8987.
de Groot, R.S., Wilson, M.A., Boumans, R.M.J., 2002. A typology for the classification, description and valuation of ecosystem functions, goods and services. Ecol. Econ. 41, 393–408.
Defries, R.S., Foley, J.A., Asner, G.P., 2004. Land-use choices: Balancing human needs and ecosystem function. Front. Ecol. Environ. 2, 249–257.
Deng, J., 1989. Introduction to grey system theory. J. grey Syst. 1, 1–24.
Du, N., Ottens, H., Sliuzas, R., 2010. Spatial impact of urban expansion on surface water bodies — A case study of 94, 175–185. doi:10.1016/j.landurbplan.2009.10.002.
Eigenbrod, F., Armsworth, P.R., Anderson, B.J., Heinemeyer, A., Gillings, S., Roy, D.B., Thomas, C.D., Gaston, K.J., 2010. The impact of proxy-based methods on mapping the distribution of ecosystem services. J. Appl. Ecol. 47, 377–385.
Foley, J.A., Defries, R.S., Asner, G.P., Barford, C., Bonan, G., Carpenter, S.R., Chapin, F.S., Coe, M.T., Daily, G.C., Gibbs, H.K., 2005. Global Consequences Land Use. Science 309 (80), 570–574.
Fu, B., Li, Y., Wang, Y., Zhang, B., Yin, S., Zhu, H., Xing, Z., 2016. Evaluation of ecosystem service value of riparian zone using land use data from 1986 to 2012. Ecol. Indic. 69, 873–881.
Haase, D., Schwarz, N., Strohbach, M., Kroll, F., Seppelt, R., 2012. Synergies, trade-offs, and losses of ecosystem services in urban regions: an integrated multiscale framework applied to the leipzig-halle region, Germany. Ecol. Soc. 17.
Hu, Y., Zheng, Y., Zheng, X., 2013. Simulation of land-use scenarios for Beijing using CLUE-S and Markov composite models. Chin. Geogr. Sci. 23, 92–100. https://doi.org/10.1007/s11769-013-0594-9.
Hwang, T., Song, C., Bolstad, P.V., Band, L.E., 2011. Downscaling real-time vegetation dynamics by fusing multi-temporal MODIS and Landsat NDVI in topographically complex terrain. Rem. Sensi. Environ. 115, 2499–2512.
Lawler, J.J., Lewis, D.J., Nelson, E., Plantinga, A.J., Polasky, S., Withey, J.C., Helmers, D.P., Martinuzzi, S., Pennington, D., Radeloff, V.C., 2014. Projected land-use change impacts on ecosystem services in the United States. Proc. Natl. Acad. Sci. U.S.A. 111, 7492–7497. https://doi.org/10.1073/pnas.1405557111.
Li, X.M., Xiao, R.B., Yuan, S.H., Chen, J.A., Zhou, J.X., 2010. Urban total ecological footprint forecasting by using radial basis function neural network: A case study of Wuhan city. China. Ecol. Indic. 10, 241–248. https://doi.org/10.1016/j.ecolind.2009.05.003.
Li, X., Wang, Y., Li, J., Lei, B., 2016. Physical and Socioeconomic Driving Forces of Land-Use and Land-Cover Changes: A Case Study of Wuhan City, China. Disc. Dynam. Nat. Soc. 2016, 1–11.
Lin, T., Xue, X., Shi, L., Gao, L., 2013. Urban spatial expansion and its impacts on island ecosystem services and landscape pattern: a case study of the island city of Xiamen, Southeast China. Ocean Coast. Manage. 81, 90–96. https://doi.org/10.1016/j.ocecoaman.2012.06.014.
Liu, J., Liu, M., Zhuang, D., Zhang, Z., Deng, X., 2013. Study on spatial pattern of land-use change in China during 1995–2000. Sci. China Ser. D Earth Sci. 46, 373–384. https://doi.org/10.1360/03yd9033.
Liu, X., Li, X., Liu, L., He, J., Ai, B., 2008. A bottom-up approach to discover transition rules of cellular automata using ant intelligence. Int. J. Geogr. Inf. Sci. 22, 1247–1269. https://doi.org/10.1080/13658810701757510.
Liu, Y., Li, J., Zhang, H., 2012. An ecosystem service valuation of land use change in Taiyuan City. China. Ecol. Modell. 225, 127–132. https://doi.org/10.1016/j.ecolmodel.2011.11.017.
Liu, Y., Ming, D., Yang, J., 2002. Optimization of land use structure based on ecological GREEN equivalent. Geo-spatial Inf. Sci. 5, 60–67. https://doi.org/10.1007/BF02826478.
Liu, Y., Tang, W., He, J., Liu, Y., Ai, T., Liu, D., 2015a. A land-use spatial optimization model based on genetic optimization and game theory. Comput. Environ. Urban Syst. 49, 1–14. https://doi.org/10.1016/j.compenvurbsys.2014.09.002.
Liu, Y., Luo, T., Liu, Z., Kong, X., Li, J., Tan, R., 2015b. A comparative analysis of urban and rural construction land use change and driving forces: implications for urban-rural coordination development in Wuhan. Central China Habitat Int. 47, 113–125. https://doi.org/10.1016/j.habitatint.2015.01.012.
Lu, M., Tang, X., Wang, Z., Gbaguidi, A., Liang, S., Hu, K., Wu, L., Wu, H., Huang, Z., Shen, L., 2017. Source tagging modeling study of heavy haze episodes under complex regional transport processes over Wuhan megacity, Central China. Environ. Pollut. 231, 612–621. https://doi.org/10.1016/j.envpol.2017.08.046.
Marcotullio, P., Lee, Y.-S., 2003. Urban environmental transitions and urban transportation systems: a comparison of the North American and Asian experiences. Int. Dev. Plan. Rev. 25, 325–354. https://doi.org/10.3828/idpr.25.4.2.
Martínez-Harms, M.J., Balvanera, P., 2012. Methods for mapping ecosystem service supply: a review. Int. J. Biodivers. Sci. Ecosyst. Serv. Manage. 8, 17–25. https://doi.org/10.1080/21513732.2012.663792.
Martínez-Harms, M.J., Quijas, S., Merenlender, A.M., Balvanera, P., 2016. Enhancing ecosystem services maps combining field and environmental data. Ecosyst. Serv. 22, 32–40.
Mathur, O.P., 2005. Impact of globalization on cities and city-related policies in India, in: Globalization and Urban Development. Springer-Verlag, Berlin/Heidelberg pp. 43–58 doi: 10.1007/3-540-28351-X_4.
MEA, 2005. Ecosystems and human well-being: Synthesis. Island, Washington, DC. https://doi.org/10.1196/annals.1439.003.
National Development and Reform Commission (NDRC), 2016. National Agricultural Statistics on Agricultural products' cost and income 2016.
Newbold, T., Hudson, L.N., Hill, S.L.L.L., Contu, S., Lysenko, I., Senior, R.A., Börger, L., Bennett, D.J., Choimes, A., Collen, B., Day, J., De Palma, A., Díaz, S., Echeverria-Londoño, S., Edgar, M.J., Feldman, A., Garon, M., Harrison, M.L.K.K., Alhusseini, T., Ingram, D.J., Itescu, Y., Kattge, J., Kemp, V., Kirkpatrick, L., Kleyer, M., Correia, D.L.P., Martin, C.D., Meiri, S., Novosolov, M., Pan, Y., Phillips, H.R.P.P., Purves, D.W., Robinson, A., Simpson, J., Tuck, S.L., Weiher, E., White, H.J., Ewers, R.M., MacE, G.M., Scharlemann, J.P.W.W., Purvis, A., 2015. Global effects of land use on local terrestrial biodiversity. Nature 520, 45–50. https://doi.org/10.1038/nature14324.
Overmars, K.P., De Koning, G.H.J., Veldkamp, A., 2003. Spatial autocorrelation in multi-scale land use models. Ecol. Modell. 164, 257–270. https://doi.org/10.1016/S0304-3800(03)00070-X.
Plummer, M.L., 2009. Assessing benefit transfer for the valuation of ecosystem services. Front. Ecol. Environ. 7, 38–45.
Rodríguez, J., Beard Jr, T.D., Bennett, E.M., Cumming, G., Cork, S., Agard, J., Dobson, A., Peterson, G., 2006. Trade-offs across space, time, and ecosystem services. Ecol. Soc. 11.
Sadeghi, S.H.R., Jalili, K., Nikkami, D., 2009. Land use optimization in watershed scale. Land Use Policy 26, 186–193. https://doi.org/10.1016/j.landusepol.2008.02.007.
Song, W., Deng, X., Yuan, Y., Wang, Z., Li, Z., 2015. Impacts of land-use change on valued ecosystem service in rapidly urbanized North China Plain. Ecol. Modell. 318, 245–253.
Turner, K.G., Odgaard, M.V., Bøcher, P.K., Dalgaard, T., Svenning, J.-C., 2014. Bundling ecosystem services in Denmark: trade-offs and synergies in a cultural landscape. Landsc. Urban Plan. 125, 89–104.
Verburg, P.H., de Nijs, T.C.M.M., Ritsema Van Eck, J., Visser, H., de Jong, K., 2004. A method to analyse neighbourhood characteristics of land use patterns. Comput. Environ. Urban Syst. 28, 667–690. https://doi.org/10.1016/j.compenvurbsys.2003.07.001.
Verburg, P.H., Eickhout, B., van Meijl, H., 2008. A multi-scale, multi-model approach for analyzing the future dynamics of European land use. Ann. Reg. Sci. 42, 57–77.
Verburg, P.H., Koomen, E., Hilferink, M., Pérez-Soba, M., Lesschen, J.P., 2012. An assessment of the impact of climate adaptation measures to reduce flood risk on ecosystem services. Landsc. Ecol. 27, 473–486.
Verburg, P.H., Overmars, K., 2009. Combining top-down and bottom-up dynamics in land use modeling: exploring the future of abandoned farmlands in Europe with the Dyna-CLUE model. Landsc. Ecol. 24, 1167–1181. https://doi.org/10.1007/s10980-009-9355-7.
Verburg, P.H.P., Soepboer, W., Veldkamp, A., Limpiada, R., Espaldon, V., Mastura, S.S.A., 2002. Modeling the spatial dynamics of regional land use: the CLUE-S model. Env. Manage. 30, 391–405. https://doi.org/10.1007/s00267-002-2630-x.
Wackernagel, M., Onisto, L., Bello, P., Linares, a C., Falfan, I.S.L., Garcia, J.M., Guerrero, a.I.S., Guerrero, M.G.S., 1999. National natural capital accounting with the ecological footrpint concept. Ecol. Econ. 29, 375–390.
Wang, G., Jiang, G., Zhou, Y., Liu, Q., Ji, Y., Wang, S., Chen, S., Liu, H., 2007. Biodiversity conservation in a fast-growing metropolitan area in China: A case study of plant diversity in Beijing. Biodivers. Conserv. 16, 4025–4038. https://doi.org/10.1007/s10531-007-9205-3.

Wang, S., Wang, X., Zhang, H., 2015. Simulation on optimized allocation of land resource based on DE-CA model. Ecol. Modell. 314, 135–144. https://doi.org/10.1016/j.ecolmodel.2015.07.011.
Wang, Y., Li, X., Li, J., 2014. Study on the Response of Ecological Capacity to Land-Use/Cover Change in Wuhan City: A Remote Sensing and GIS Based Approach. doi:10.1155/2014/794323.
Wu, J., 2011. Studies on the evolution of use patten of lakeshores in wuhan. Adv. Mater. Res. 250–253, 3554–3558. https://doi.org/10.4028/www.scientific.net/AMR.250-253.3554.
Wuhan Forestry Bureau (WFB), 2016. The 13th Five-Year Plan for Gardens and Forestry Development of Wuhan City (2016-2020).
Wuhan Land Resources and Planning Bureau (WLRPB), 2012. Three Lines and One Road Protection Plan for Lakes in Central District of Wuhan City.
Wuhan Land Resources and Planning Bureau (WLRPB), 2011. Land Use Planning of Wuhan City (2006-2020).
Xie, G., Lu, C., Leng, Y., Zheng, D., Li, S., 2003. Ecological assets valuation of the Tibetan Plateau (in Chinese). J. Nat. Resour. 18, 189–196.
Xie, G., Zhen, L., Lu, C., Xiao, Y., Chen, C., 2008. Expert knowledge based valuation method of ecosystem services in China (in Chinese). J. Nat. Resour. 23, 911–919.
Xin, L., Wang, J., Wang, L., 2015. Prospect of per capita grain demand driven by dietary structure change in China (in Chinese). Resour. Sci. 37, 1347–1356.
Zhang, L., Nan, Z., Yu, W., Ge, Y., 2015. Modeling land-use and land-cover change and hydrological responses under consistent climate change scenarios in the Heihe River Basin, China. . Water Resour. Manage. 29, 4701–4717.